THE JOURNAL OF BIOLOGICAL CHEMISTRY VOL. 283, NO. 43, pp. 29175–29185, October 24, 2008

Protein-tyrosine Phosphatase α Regulates Stem Cell Factor-dependent c-Kit Activation and Migration of Mast Cells*

Received for publication, May 28, 2008, and in revised form, August 7, 2008 Published, JBC Papers in Press, August 25, 2008, DOI 10.1074/jbc.M804077200

Lionel A. Samayawardhena[‡§] **and Catherine J. Pallen**[‡§¶1]

From the Departments of [‡]*Pediatrics and* [¶]*Pathology and Laboratory Medicine and the* [§]*Child and Family Research Institute, University of British Columbia, Vancouver, British Columbia V5Z 4H4, Canada*

The role of protein-tyrosine phosphatase α (PTPα) in mast cell function was investigated in tissues and cells from PTPα-deficient mice. Bone marrow-derived mast cells (BMMCs) lacking PTPα exhibit defective stem cell factor (SCF)-dependent polarization and migration. Investigation of the molecular basis for this reveals that SCF/c-Kit-stimulated activation of the Fyn tyrosine kinase is impaired in PTPα$^{-/-}$ BMMCs, with a consequent inhibition of site-specific c-Kit phosphorylation at tyrosines 567/569 and 719. Although c-Kit-mediated activation of phosphatidylinositol 3-kinase and Akt is unaffected, profound defects occur in the activation of downstream signaling proteins, including mitogen-activated protein kinases and Rho GTPases. Phosphorylation and interaction of Fyn effectors Gab2 and Shp2, which are linked to Rac/JNK activation in mast cells, are impaired in PTPα$^{-/-}$ BMMCs. Thus, PTPα is required for SCF-induced c-Kit and Fyn activation, and in this way regulates a Fyn-based c-Kit signaling axis (Fyn/Gab2/Shp2/Vav/PAK/Rac/JNK) that mediates mast cell migration. These defective signaling events may underlie the altered tissue-resident mast cell populations found in PTPα$^{-/-}$ mice.

PTPα[2] is a receptor-type protein-tyrosine phosphatase that is widely expressed in many cells and tissues including those of hematopoietic origin. It has a short, glycosylated extracellular region with no known ligand binding specificity, a single transmembrane spanning region, and an intracellular region containing two tandem catalytic domains (1). The generation of PTPα-deficient mice confirmed findings from PTPα overexpression studies that this phosphatase functions as a physiological regulator of Src family kinases (SFKs), catalyzing the dephosphorylation of the inhibitory C-terminal tyrosine residue of SFKs and activating them (2–5). Despite the widespread actions of SFKs in multiple cellular and biological processes, PTPα-null mice with reduced SFK activity are viable and have an overall normal appearance, suggesting that PTPα is likely one of several SFK regulators with tissue-, cell-, and/or signaling pathway-specific functions.

In keeping with PTPα being highly expressed in brain, several studies, many utilizing PTPα-null mice and cells, have revealed multiple cellular and/or physiological roles of this PTP linked to nervous system development and function. These include regulating *N*-methyl-D-aspartate receptor phosphorylation and activity, long-term potentiation, and spatial memory (6–9); sciatic nerve myelination and voltage-gated potassium channel activation and phosphorylation (10, 11), migration of pyramidal neurons (6), and neuronal outgrowth and differentiation (3, 12–15). In addition, PTPα regulates integrin-stimulated cell migration (4, 16), T cell activation (17), and mitosis (18). In the absence of an identified ligand for PTPα, it appears that PTPα-mediated SFK activation is often linked to activation of certain receptors by their ligands. Indeed, PTPα physically associates with receptors that themselves lack enzymatic activity, including the neural cell adhesion molecules contactin and NCAM140 (12, 19), and integrin α_v (20), and in this way may mediate ligand-induced SFK activation.

Cells of the immune system have multiple well defined signaling pathways that are initiated by receptor-mediated SFK-dependent events. A role for PTPα has been recently demonstrated in T cell receptor-mediated activation and CD44-mediated spreading of T cells (17, 21). To further our understanding of PTPα functions in immune cells, and also to query whether PTPα regulates SFK-dependent signaling that is initiated by a receptor with intrinsic enzymatic activity, we have investigated the role of PTPα in mast cells, and specifically in regulating signaling by the receptor-tyrosine kinase c-Kit.

Mast cells play key roles in innate and adaptive immune responses, extending from their actions as regulators of allergic inflammation to roles in host defense, immunological tolerance and autoimmune diseases, atherosclerosis, and cancer (22–24). Mast cell progenitors leave the bone marrow and migrate to various connective and mucosal locations where they complete their development and give rise to mature populations with tissue-specific functions (25, 26). Many mast cell processes such as migration, proliferation, survival, differentiation, and maturation are regulated by stem cell factor (SCF) (27). This ligand binds to and activates c-Kit, a member of the type III subclass of receptor tyrosine kinases. Besides its role in normal mast cell development and function, aberrant c-Kit signaling, due to c-Kit overexpression, or autocrine or mutational activation, is linked to mastocytosis and some human tumors such as

* This work was supported in part by Canadian Institutes of Health Research Grant MOP-49410. The costs of publication of this article were defrayed in part by the payment of page charges. This article must therefore be hereby marked "*advertisement*" in accordance with 18 U.S.C. Section 1734 solely to indicate this fact.

[1] Recipient of an investigator award from the Child and Family Research Institute. To whom correspondence should be addressed: 3102-950 West 28th Ave., Vancouver, BC V5Z 4H4, Canada. Tel.: 604-875-2439; Fax: 604-875-2417; E-mail: cpallen@interchange.ubc.ca.

[2] The abbreviations used are: PTPα, protein-tyrosine phosphatase α; BMMC, bone marrow-derived mast cell; MSCV, murine stem cell virus; SCF, stem cell factor; SFK, Src family kinase; PI3K, phosphatidylinositol 3-kinase; ERK, extracellular signal-regulated kinase; JNK, c-Jun N-terminal kinase; PE, phycoerythrin; IL, interleukin; GST, glutathione *S*-transferase; PBD, p21-binding domain; FACS, fluorescence-activated cell sorter.

acute myeloid leukemia and gastrointestinal stromal tumors (28–30). The development of therapeutics targeted to c-Kit or to c-Kit regulators and signaling effectors is being actively pursued for the treatment of these diseases.

The earliest events in c-Kit-mediated signaling are the SCF-induced trans-autophosphorylation of receptor dimers, creating phosphotyrosyl binding sites for several signaling molecules. Extensive mutation/function analyses of c-Kit have identified phosphorylated tyrosine residues and their binding partners that are critical in SCF-dependent cell events and processes. For example, three tyrosine residues, Tyr^{567}, Tyr^{569}, and Tyr^{719}, are responsible for c-Kit-mediated cell migration, with $Tyr^{567/569}$ playing a more critical role in this process (31, 32). Phospho-$Tyr^{567/569}$ is a binding site for the SFKs Fyn (33, 34) and Lyn (35, 36), and recruitment of these kinases by c-Kit is believed to effect their activation. In addition, the phosphatases Shp1 and Shp2, as well as Chk, Cbl, Shc, and APS can associate with phospho-$Tyr^{567/569}$, phospho-Tyr^{719} recruits phosphatidylinositol 3-kinase (PI3K), and other phosphorylated tyrosine residues bind to proteins such as Grb2, Grb7, and phospholipase γ (37, 38). The complexes of phosphotyrosyl-c-Kit and associated molecules activate multiple downstream signaling events that determine mast cell responses. Critical roles for the c-Kit upstream effectors Fyn, Lyn, or the p85 subunit of class 1_A PI3K are apparent from the multiple defective SCF-stimulated signaling events and responses of mast cells lacking these molecules (39–43).

We find that bone marrow-derived mast cells (BMMCs) from PTP$\alpha^{-/-}$ mice have profound defects in c-Kit-dependent migration, and c-Kit signaling is impaired at multiple points. Notable early defects involve defective Fyn activation and c-Kit tyrosine phosphorylation that impinge on Gab2-mediated downstream events such as Rac/JNK activation, whereas PI3K/Akt signaling from c-Kit is unaffected. Also, tissue-resident mast cell populations are altered in PTPα-null mice. Thus, the cooperative interaction of two receptors with opposing enzymatic activities, the receptor tyrosine kinase c-Kit and the RPTP PTPα, is required for SCF-stimulated SFK activation and signaling, and for mast cell migration.

EXPERIMENTAL PROCEDURES

Animals—PTP$\alpha^{-/-}$ and wild-type (PTP$\alpha^{+/+}$) mice (5) were maintained as an advanced intercross line (129*SvEv* x Black Swiss, 50:50 mixed background) and housed under specific pathogen-free conditions. Animal care and use followed the guidelines of the University of British Columbia and the Canadian Council on Animal Care.

Antibodies and Reagents—The following antibodies were used: c-Kit, phospho-Tyr^{719}-c-Kit, phospho-Ser^{473}-Akt, Akt, phospho-Tyr^{507}-Lyn, Lyn, Fyn, phospho-ERK1/2, ERK1/2, phospho-$Thr^{180/182}$-p38, p38, phospho-JNK, JNK, phospho-Tyr^{542}-Shp2, phospho-Tyr^{452}-Gab2, phospho-PAK (Cell Signaling Technology); Fyn, Shp2 (BD Biosciences); phospho-$Tyr^{567/569}$-c-Kit, Shc, Vav, PAK, actin (Santa Cruz Biotechnology); phosphotyrosine (4G10), Gab2, p85, Rac2 (Upstate Biotechnology); phospho-Tyr^{529}-Src (BIOSOURCE), Rac1 (Stressgen), Cdc42 (Chemicon), dinitrophenyl-IgE (Sigma), IgE-fluorescein isothiocyanate, c-Kit-phycoerythrin (PE), rat IgG_1-fluorescein isothiocyanate, rat $IgG2_b$-PE (Caltag Labs). Alexa Fluor 488-conjugated phalloidin was purchased from Molecular Probes. Horseradish peroxidase-conjugated goat anti-mouse antibody and horseradish peroxidase-conjugated goat anti-rabbit antibody were from Sigma. Recombinant SCF, IL-3, and IL-6 were purchased from PeproTech, Inc. SU6656 was from EMD Biosciences.

Analysis of Tissue Resident Mast Cell Populations—Paraformaldehyde-fixed skin samples from mouse ears and backs, and sections from stomachs, were stained with toluidine blue, and the mast cells visualized by microscopy and counted. Peritoneal cells were recovered by lavage and kept at 37 °C overnight in BMMC medium (Iscove's modified Dulbecco's medium with 10% fetal bovine serum, 1% antimicrobial-antimycotic, 1 mM sodium pyruvate, 1% non-essential amino acids, 50 μM α-monothioylglycolate) containing 100 ng/ml dinitrophenyl-IgE. Cells were washed in phosphate-buffered saline and labeled with anti-IgE-fluorescein isothiocyanate and anti-kit-PE, or with the isotype controls rat IgG_1-fluorescein isothiocyanate and rat $IgG2_b$-PE, and analyzed by flow cytometry. Mast cell (double labeled for FcεRI and c-Kit) numbers were determined and their percentage of the total cells was calculated. Alternatively, cells from peritoneal lavages were washed and resuspended in cold phosphate-buffered saline, fixed in 4% paraformaldehyde at 4 °C overnight, and then stained with toluidine blue for mast cell counting.

Isolation, Culture, and Characterization of BMMCs—Bone marrow from femurs of 4–8-week-old PTP$\alpha^{+/+}$ and PTP$\alpha^{-/-}$ mice was placed in BMMC medium containing IL-3. The IL-3 sources were 3–5% conditioned medium from X63-IL-3 cells (kindly provided by Dr. A. Craig, Queens University) or from WEHI-3 cells (kindly provided by Dr. K. McNagny, University of British Columbia), or 10 ng/ml recombinant mouse IL-3. BMMCs were enriched by discarding adherent cells. The isolated BMMCs were maintained in culture at 0.5–1.0 × 10^6 cells/ml for 4–6 weeks. Before use, BMMC purity was routinely monitored by flow cytometry to detect c-Kit and FcεRI.

Plasmid Constructs and BMMC Infection—PTPα cDNA was cloned into BglII and XhoI sites in pMSCVpuro vector (Clontech Laboratories, Inc.) and the insert verified by sequencing. The PT67 murine stem cell virus (MSCV) packaging cell line was transfected with pMSCVpuro or pMCSVpuro-PTPα plasmids using Lipofectamine, and retroviruses collected 48 h later and filtered (0.2 μm pore). Bone marrow cells from PTPα-null mice were cultured in BMMC medium containing 10 ng/ml IL-6, 10 ng/ml IL-3, and 50 ng/ml SCF for 4 days. The bone marrow progenitors were incubated twice with retroviral supernatants in media with 8 μg/ml Polybrene for 24 h. Cells were cultured in BMMC media for 2 days, followed by selection with 1 μg/ml puromycin for 3 weeks, and analyzed by flow cytometry to confirm the surface expression of c-Kit and FcεRI prior to use.

BMMC Spreading, Polarization, and Migration—BMMCs were placed in starvation medium (BMMC medium without IL-3) overnight. To assess spreading and polarization, the cells were plated on fibronectin (20 μg/ml)-coated glass coverslips in Iscove's modified Dulbecco's medium with 0.1% bovine serum albumin with or without 50 ng/ml SCF. After 15 or 60 min, the

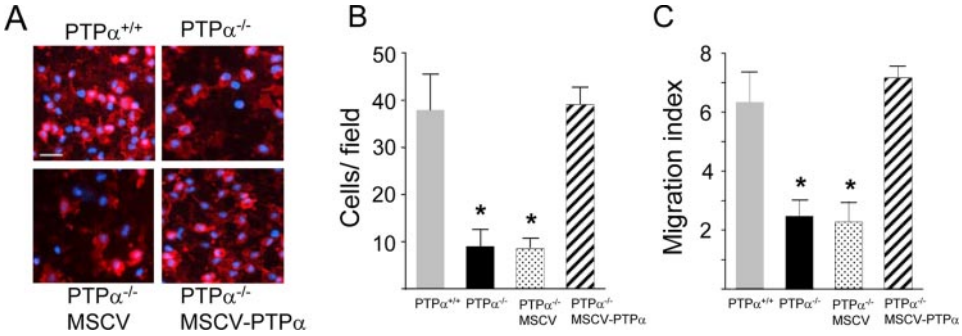

FIGURE 1. **SCF-induced migration is impaired in PTPα$^{-/-}$ BMMCs.** PTPα$^{+/+}$ and PTPα$^{-/-}$ BMMCs, and PTPα$^{-/-}$ BMMCs that had been infected with MSCV bearing empty vector (*MSCV*) or a PTPα expression vector (*MSCV-PTPα*) were placed in Transwell inserts and their migration toward the bottom chambers containing 25 ng/ml SCF was determined. *A*, at 60 min, BMMCs attached to the underside of the filters were fixed and stained with 4′,6-diamidino-2-phenylindole (*blue*) and phalloidin (*red*) (*scale bar*, 25 μm). *B*, the numbers of 4′,6-diamidino-2-phenylindole-stained nuclei on the undersides of filters were counted after 60 min migration, and the cell number ± S.D. calculated. *C*, at 90 min, the numbers of cells that had migrated into the medium in the bottom chamber were counted, and used to calculate the migration index ± S.D. Experiments were performed 3–4 times, each time with BMMCs derived from different pairs of PTPα$^{+/+}$ and PTPα$^{-/-}$ mice. Each experiment utilized 3–5 Transwells/genotype. *Asterisks* denote significant differences ($p < 0.0001$) between the PTPα$^{+/+}$ (wild-type) BMMCs and the PTPα-null or retrovirally infected BMMCs.

cells were fixed in 4% paraformaldehyde, permeabilized with 0.1% Triton X-100 in phosphate-buffered saline, labeled with Alexa-Fluor 488-conjugated phalloidin and 4′,6-diamidino-2-phenylindole, and visualized using a Leica DM4000 B microscope. Cell length and area were quantified using Open Lab 4.0.2 software. For migration assays, the starved BMMCs were resuspended in Iscove's modified Dulbecco's medium with 0.1% bovine serum albumin, and 4×10^5 cells were placed in the upper well of a Transwell chamber (Costar, 3 μm pore). The lower chamber contained 0.5 ml of migration medium with or without 25 ng/ml SCF. After incubation at 37 °C for 60 or 90 min, non-migratory cells on the membrane upper surface were removed with a cotton swab, and the migrated cells on the bottom surface of the membrane were fixed, permeabilized, and labeled as above. Cells were visualized by fluorescence microscopy, and the number of cells per field counted for 6 fields/membrane. BMMCs that had migrated into the medium in the lower well were counted and the migration index ((number of cells migrated/number of cells seeded) × 100) was calculated.

BMMC Stimulation and Lysis—BMMCs were placed overnight in starvation medium, washed once in starvation medium, and resuspended in prewarmed Tyrodes buffer (10 mM Hepes, pH 7.4, 130 mM NaCl, 5 mM KCl, 1.4 mM $CaCl_2$, 1 mM $MgCl_2$, 5.6 mM glucose, 0.1% bovine serum albumin). BMMCs were stimulated with or without 100 ng/ml recombinant mouse SCF and incubated at 37 °C. Stimulation was stopped with cold phosphate-buffered saline with 0.1 mM Na_3VO_4. Cells were pelleted by centrifugation at 4 °C and solubilized in lysis buffer (20 mM Tris-HCl, pH 7.5, 150 mM NaCl, 1 mM EDTA, 1% Nonidet P-40, 0.5% sodium deoxycholate, 1 mM Na_3VO_4, 10 μg/ml aprotinin, 10 μg/ml leupeptin, 100 μM phenylmethylsulfonyl fluoride) for 30 min at 4 °C. Insoluble material was removed by centrifugation at 12,000 × *g* for 15 min to generate soluble cell lysates. Signals from immunoblotting were quantified by densitometric scanning and analysis using Quantity One software (Bio-Rad).

Rac and Cdc42 Activation Assays—BMMCs were unstimulated or stimulated with SCF as described above and lysed in 50 mM Tris-HCl, pH 7.5, 150 mM NaCl, 1% Triton X-100, 0.25% sodium deoxycholate, 10% glycerol, 25 mM NaF, 10 mM $MgCl_2$, 1 mM EDTA, 1 mM sodium orthovanadate, 10 μg/ml aprotinin, 10 μg/ml leupeptin. Lysates were incubated for 60 min at 4 °C on a rotator with glutathione *S*-transferase-p21-binding domain (GST-PBD) fusion protein pre-bound to glutathione-Sepharose beads. GST-PBD-bound complexes were recovered by centrifugation followed by three washes with lysis buffer.

Data Analysis—Cell polarization and migration data and that obtained by densitometric quantification of immunoblots were statistically analyzed using single factor analysis of variance and/or the Student's *t* test.

RESULTS

Impaired SCF-induced Migration of PTPα$^{-/-}$ BMMCs—BMMC progenitor cells were prepared and cultured in the presence of conditioned medium containing the cytokine IL-3. After 4 weeks of culture, FACS analyses determined that >97% of the PTPα$^{-/-}$ and wild-type cells ($n = 10$ independent cultures/genotype) were positive for both c-Kit and FcεR1, markers of mature mast cells (data not shown). Thus PTPα is not required for IL-3-induced mast cell maturation *ex vivo*.

A Transwell chemotaxis assay was used to investigate the requirement for PTPα in mast cell migration that is mediated by signaling by the SCF receptor (c-Kit) and integrins (44). Compared with wild-type BMMCs, a significant reduction (~80%) was observed in the number of PTPα-deficient BMMCs that migrated to the underside of the membrane (Fig. 1, *A* and *B*), and into the SCF-containing medium in the bottom chambers of the wells (Fig. 1*C*). In the absence of SCF, very few BMMCs of either genotype migrated to the underside of the membrane (PTPα$^{+/+}$, 1.7 ± 0.8/field; PTPα$^{-/-}$, 2.1 ± 1.2/field), and no cells were found in the medium of the bottom chambers (data not shown), indicating that the SCF receptor, c-Kit, was functionally involved in mediating the above responses. To confirm that the absence of PTPα was the underlying cause of this migration defect, PTPα was re-expressed in the PTPα-null BMMCs by retroviral (MSCV) infection, to a level equivalent to 138% of that in wild-type BMMCs. This completely restored the SCF-dependent migration ability of the mast cells, whereas infection with retrovirus expressing a control "empty" vector was unable to rescue impaired migration of PTPα$^{-/-}$ BMMCs (Fig. 1, *A–C*).

PTPα$^{-/-}$ BMMCs Exhibit Delayed Spreading and Polarization—In view of the migration defect of PTPα$^{-/-}$ BMMCs, their ability to carry out several cellular events associated with cell migration was investigated. BMMCs were

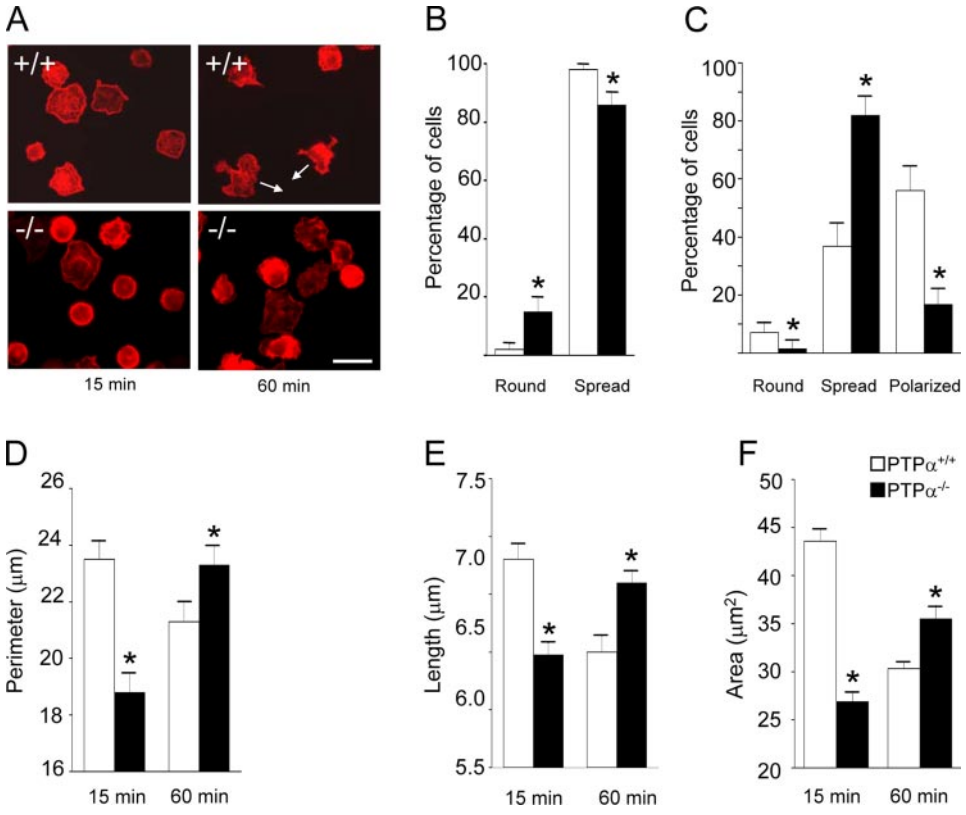

FIGURE 2. **Delayed SCF-induced spreading and polarization of PTP$\alpha^{-/-}$ BMMCs.** PTP$\alpha^{+/+}$ (+/+) and PTP$\alpha^{-/-}$ (−/−) BMMCs were plated on fibronectin-coated coverslips in medium with 50 ng/ml SCF. After 15 and 60 min, cells were fixed and stained with phalloidin, and morphology and associated parameters were scored. *A*, representative photographs of cells. *Arrows* indicate directionality of polarized cells. *Scale bar*, 10 μm. *B*, percentages (mean ± S.D.) of round or spread cells at 15 min ($n = 30$). *C*, percentages (mean ± S.D.) of round, spread, or polarized cells at 60 min ($n = 30$). *D*, cell perimeter; *E*, cell length at the longest axis; and *F*, cell area were measured at 15 and 60 min and the mean ± S.E. are shown ($n = 200$). In *B–F*, data were collected from three independent experiments. *White bars* represent PTP$\alpha^{+/+}$ BMMCs and *black bars* represent PTP$\alpha^{-/-}$ BMMCs, and *asterisks* depict a significant difference ($p < 0.05$) between cell types.

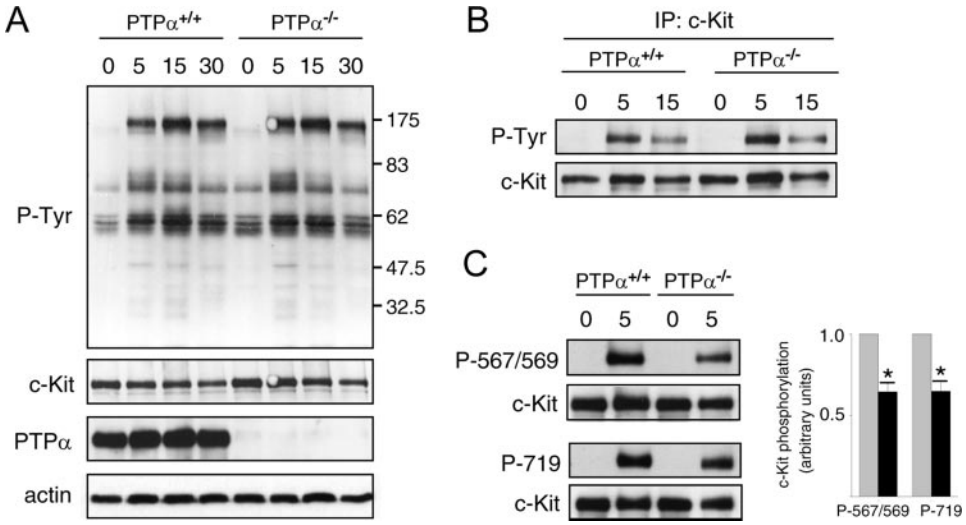

FIGURE 3. **SCF-stimulated tyrosine phosphorylation of BMMC proteins and c-Kit in wild-type and PTP$\alpha^{-/-}$ cells.** Wild-type (PTP$\alpha^{+/+}$) and PTP$\alpha^{-/-}$ BMMCs were left untreated (0) or stimulated with SCF for 5, 15, and 30 min. *A*, cell lysates were probed for phosphotyrosine (*P-Tyr*), c-Kit, PTPα, and actin as indicated. *B*, c-Kit was immunoprecipitated and probed for phosphotyrosine and c-Kit. The immunoblots shown in *A* and *B* are representative of results of 6–8 independent experiments. *C*, cell lysates without or with 5 min SCF treatment were probed with phosphosite-specific c-Kit antibodies and anti-c-Kit antibody. Results from three experiments were quantified and are shown in the *graph*. *Bars* represent the mean ± S.D. (*gray*, PTP$\alpha^{+/+}$ cells; *black*, PTP$\alpha^{-/-}$ cells). The *asterisks* depict a significant difference ($p < 0.01$).

plated on fibronectin-coated dishes in the presence of SCF. No difference in the attachment of wild-type and PTP$\alpha^{-/-}$ cells was observed (data not shown). At 15 and 60 min after plating, cells were scored as round or spread, with the additional phenotype of a polarized appearance being scored at 60 min (Fig. 2*A*). At 15 min, a higher percentage of PTP$\alpha^{-/-}$ cells than wild-type cells were round, and a lower percentage of PTP$\alpha^{-/-}$ cells than wild-type cells had spread (Fig. 2*B*). At 60 min, the situation was reversed, and notably, whereas 81.9% (± 1.2 S.D.) of PTP$\alpha^{-/-}$ cells were spread, only 36.9% (±1.5 S.D.) of wild-type cells were spread. However, many more of the wild-type cells than PTP$\alpha^{-/-}$ BMMCs had progressed to a polarized phenotype at this time (56.0 ± 1.6% S.D. *versus* 16.7 ± 1.0% S.D., respectively) (Fig. 2*C*). Overall, these results indicate that PTP$\alpha^{-/-}$ BMMCs exhibit delayed SCF- and integrin-mediated spreading and polarization. Cell morphological parameters were also quantified. Consistent with phenotypic observations, PTP$\alpha^{-/-}$ BMMCs had a shorter perimeter and length than wild-type BMMCs at 15 min (Fig. 2, *D* and *E*), and this was reversed at 60 min. The cell area of PTP$\alpha^{-/-}$ BMMCs was also significantly smaller than that of wild-type BMMCs at 15 min, indicative of slower PTP$\alpha^{-/-}$ cell spreading (Fig. 2*F*). At 60 min, PTP$\alpha^{-/-}$ BMMCs had a larger cell area than wild-type BMMCs (Fig. 2*F*), correlating with the higher relative percent of PTP$\alpha^{-/-}$ BMMCs that were still at the spreading stage and, unlike the wild-type BMMCs, had not yet progressed to a more compact polarized shape. Together, these observations suggest that SCF- and integrin-mediated signaling defects are manifested in cytoskeletal and cell shape remodeling that likely account for impaired PTP$\alpha^{-/-}$ BMMC migration.

PTPα-null BMMCs Have Site-specific Alterations in SCF-stimulated c-Kit Tyrosine Phosphorylation—Because impaired SCF-dependent

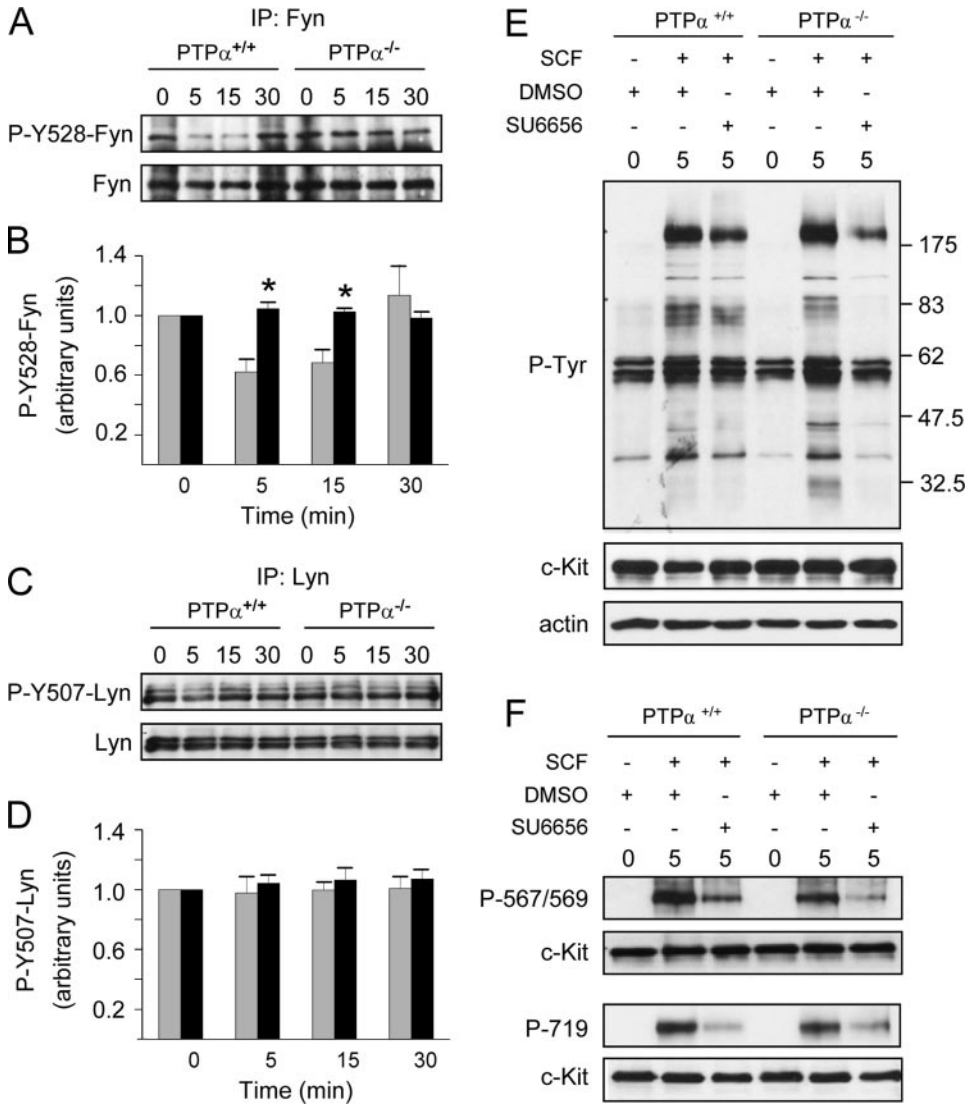

FIGURE 4. **SCF-induced tyrosine dephosphorylation of Fyn requires PTPα and may be linked to c-Kit phosphorylation.** Wild-type (PTPα$^{+/+}$) and PTPα$^{-/-}$ BMMCs were left untreated (0) or stimulated with SCF for 5, 15, and 30 min as indicated. (*A*) Fyn and (*C*) Lyn immunoprecipitates (*IP*) were immunoblotted using anti-Tyr(P)^{527}-Src antibody (*top panels*), and anti-Fyn or -Lyn as appropriate (*bottom panels*). Immunoblots were quantified by densitometry, and the C-terminal tyrosine phosphorylation of these kinases calculated per unit of (*B*) Fyn or (*D*) Lyn protein. The *bars* in *B* and *D* represent the mean ± S.D. (Fyn, $n = 6$; Lyn, $n = 3$) and the *asterisks* depict a significant difference ($p < 0.01$) between PTPα$^{+/+}$ (*gray bars*) and PTPα$^{-/-}$ (*black bars*) BMMCs. In other experiments, wild-type and PTPα$^{-/-}$ BMMCs were pretreated with DMSO or 5 μM SU6656 for 30 min, and harvested (0) or incubated with added SCF for a further 5 min. Lysates were probed for: *E*, phosphotyrosine (*P-Tyr*), c-Kit, and actin; or *F*, for phospho-Tyr$^{567/569}$ and phospho-Tyr^{719} of c-Kit, and c-Kit. Similar results were obtained in two other independent experiments.

migration of PTPα$^{-/-}$ BMMCs was observed, we investigated whether SCF-stimulated signaling events in BMMCs were affected by the absence of PTPα. No obvious differences in protein tyrosine phosphorylation profiles were apparent between wild-type and PTPα$^{-/-}$ cells following SCF stimulation for up to 30 min (Fig. 3*A*). Likewise, SCF-induced tyrosine phosphorylation of c-Kit appeared normal in BMMCs lacking PTPα (Fig. 3*B*). Despite this, probing BMMC lysates with phosphosite-specific antibodies to phospho-Tyr$^{567/569}$ and phospho-Tyr^{719} of c-Kit revealed significantly reduced (by 35%) phosphorylation at these sites after 5 min of stimulation with SCF (Fig. 3*C*), and in other experiments similar reductions were detected after 15 and 30 min stimulation (data not shown). These phosphotyrosine residues are binding sites for c-Kit effector signaling molecules, including the binding of the SFKs Fyn and Lyn to phospho-Tyr$^{567/569}$ and the recruitment of PI3K to phospho-Tyr^{719} (33–36, 45). The lowered phosphorylation of these sites in the absence of PTPα suggests that critical downstream signaling events may be impaired in PTPα$^{-/-}$ BMMCs.

Defective SCF-induced Dephosphorylation of Fyn in PTPα$^{-/-}$ BMMCs—The SFKs Lyn and Fyn are activated early in c-Kit signaling, and Fyn has specifically been implicated in SCF/c-Kit-induced, integrin-mediated BMMC spreading and polarization, whereas both Fyn and Lyn play roles in SCF/c-Kit-induced BMMC chemotaxis (39, 40, 42). Furthermore, PTPα is a positive regulator of SFKs, catalyzing their activation through dephosphorylation of the conserved regulatory C-terminal tyrosine residue (1). Therefore the tyrosine phosphorylation status of Fyn and Lyn in SCF-stimulated BMMCs was examined. In wild-type BMMCs, SCF treatment resulted in the rapid (by 5 min) dephosphorylation of Tyr^{528} of Fyn, indicative of Fyn activation (Fig. 4, *A* and *B*). The reduced phosphorylation of Fyn Tyr^{528} was maintained at 15 min, with full rephosphorylation occurring by 30 min. However, in PTPα$^{-/-}$ BMMCs, no dephosphorylation of Fyn was observed in response to SCF (Fig. 4, *A* and *B*). In contrast to Fyn, Lyn phosphorylation at the regulatory C-terminal tyrosine residue, as assessed by immunoblotting with antibody directed to phospho-Tyr^{527} of Src, was not altered upon SCF stimulation of wild-type or PTPα$^{-/-}$ BMMCs (Fig. 4, *C* and *D*). This was also the case upon probing Lyn immunoprecipitates with anti-phosphotyrosine antibody or with anti-phospho-Tyr^{507} of Lyn (data not shown). Thus we were unable to determine whether PTPα affected Lyn activity in unstimulated or SCF-stimulated BMMCs. However, the analysis of Fyn phosphorylation demonstrates that PTPα is required for SCF-stimulated Fyn dephosphorylation and the consequent activation of this SFK.

To determine whether defective SFK activity in PTPα-null BMMCs is a potential basis for the reduced SCF-stimulated phosphorylation of c-Kit Tyr$^{567/569}$ and Tyr^{719}, the phosphorylation of these sites was examined after treatment of BMMCs with the SFK inhibitor SU6656. In both wild-type and PTPα$^{-/-}$

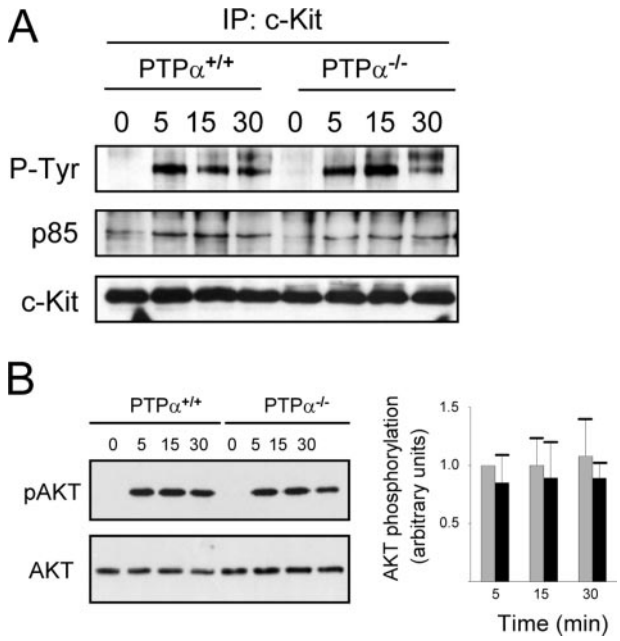

FIGURE 5. **SCF-stimulated PI3K signaling is not affected in PTPα$^{-/-}$ BMMCs.** Wild-type (PTPα$^{+/+}$) and PTPα$^{-/-}$ BMMCs were left untreated (0) or stimulated with SCF for 5, 15, and 30 min as indicated. *A*, c-Kit immunoprecipitates were probed for phosphotyrosine (*P-Tyr*), p85, and c-Kit. The blot shown is representative of three experiments, but no change in p85 binding to c-Kit was observed in two other experiments (not shown). *B*, cell lysates were probed for phospho-Ser^{473}-Akt and Akt. Quantified results from three such experiments are shown in the *graph*. The *bars* represent the mean ± S.D. and the *asterisks* depict a significant difference ($p < 0.01$) between PTPα$^{+/+}$ (*gray bars*) and PTPα$^{-/-}$ (*black bars*) BMMCs.

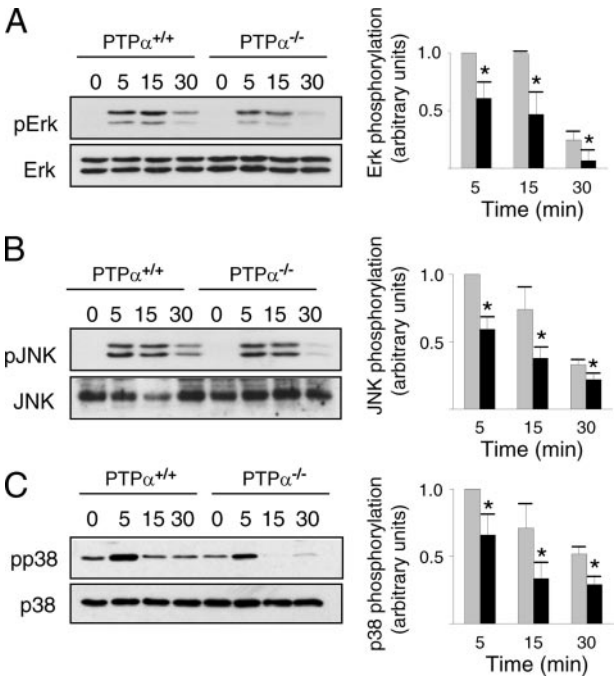

FIGURE 6. **SCF-induced MAPK activation is defective in PTPα$^{-/-}$ BMMCs.** Wild-type (PTPα$^{+/+}$) and PTPα$^{-/-}$ BMMCs were left untreated (0) or stimulated with SCF for 5, 15, and 30 min. Lysates were probed for phospho-ERK1/2 and ERK1/2 (*A*), phospho-JNK and JNK (*B*), and phospho-p38 and p38 (*C*). The results from several experiments (ERK1/2, JNK, p38, $n = 3$) were quantified by densitometry, and the mean ± S.D. are shown in the *graphs*. *Asterisks* indicate a significant difference ($p < 0.05$) between wild-type (*gray bars*) and PTPα$^{-/-}$ (*black bars*) cells.

BMMCs, this compound reduced the SCF-induced tyrosine phosphorylation of a band that co-migrated with c-Kit and of some other proteins of ~70–80 kDa (Fig. 4*E*). SU6656 also inhibited the phosphorylation of Tyr$^{567/569}$ and Tyr^{719} (Fig. 4*F*). In PTPα$^{-/-}$ BMMCs, SU6656 treatment further inhibited the already reduced phosphorylation of these residues, likely because PTPα-null cells have basal SFK activity that is lost upon SU6656 treatment. These results indicate that SFK activity is indeed required for complete c-Kit phosphorylation, and suggests that the lower phosphorylation of specific tyrosine residues of c-Kit in PTPα$^{-/-}$ BMMCs is a consequence of reduced SFK activity, including that of Fyn.

PI3K Signaling Is Not Markedly Altered in PTPα$^{-/-}$ BMMCs—PI3K binds to phospho-Tyr^{719} of c-Kit to initiate downstream signaling, including Akt activation (37, 38). Other mechanisms of c-Kit signaling can also activate PI3K, because both PI3K and Akt are activated by c-Kit lacking Tyr^{719} but with intact Tyr$^{567/569}$ residues (32). We found that binding of the p85 subunit of PI3K to c-Kit was enhanced upon SCF stimulation of wild-type and PTPα$^{-/-}$ BMMCs and that this binding was sometimes (Fig. 5*A*) but not always somewhat reduced in cells lacking PTPα. Likewise, Akt activation was not significantly different between SCF-stimulated wild-type and PTPα$^{-/-}$ BMMCs (Fig. 5*B*). Thus, c-Kit-mediated PI3K/Akt signaling is not dramatically affected in BMMCs lacking PTPα.

SCF-induced MAPK Activation Is Reduced and Less Sustained in BMMCs Lacking PTPα—Fyn and Lyn have been implicated in SCF-stimulated activation of ERK1/2, JNK, and p38 in mast cells (31, 32, 34, 39, 41). To determine whether PTPα plays a role in the activation of these MAPKs, their kinetics of activation, as reflected by site-specific changes in their phosphorylation, were compared between wild-type and PTPα-deficient BMMCs. Defects were observed in the SCF-mediated activation profiles of all of these MAPKs in PTPα-deficient BMMCs. At all times following SCF stimulation, ERK1/2 activation was reduced in cells lacking PTPα (Fig. 6*A*). JNK and p38 activation were also reduced in SCF-stimulated PTPα$^{-/-}$ cells (Fig. 6, *B* and *C*). Together, these results indicate that PTPα is required for the optimal activity of multiple downstream MAPK effectors of c-Kit signaling.

Defective Rho GTPase Activation and Signaling in PTPα$^{-/-}$ BMMCs—The Rho family of small GTPases, including the members Rho, Rac, and Cdc42, play critical roles in the migration of non-hematopoietic cells. Rac has specifically been demonstrated to mediate c-Kit signaling, as BMMCs lacking the hematopoetic cell-specific Rac2 exhibit reduced migration in response to SCF stimulation (44), Rac1 activation occurs in SCF-treated BMMCs in an SFK- and Gab2-dependent manner (46), and Rac1 and Rac2 activation is defective in Fyn-null BMMCs (40). We found that Rac1, Rac2, and Cdc42 all underwent SCF-induced activation in wild-type BMMCs, with peak activation observed between 5 and 15 min (Fig. 7, *A*–*C*). In PTPα-null BMMCs, the activation of these GTPases was delayed, with either no significant activation (Rac1, Rac2) or reduced activity (Cdc42) detected at 5 min post-SCF stimulation, and a consistent reduction in Rac1, Rac2, and Cdc42 activation that persisted from 15 to 30 min (Fig. 7, *A*–*C*). In accord with these findings, SCF-induced activation of the Rac and

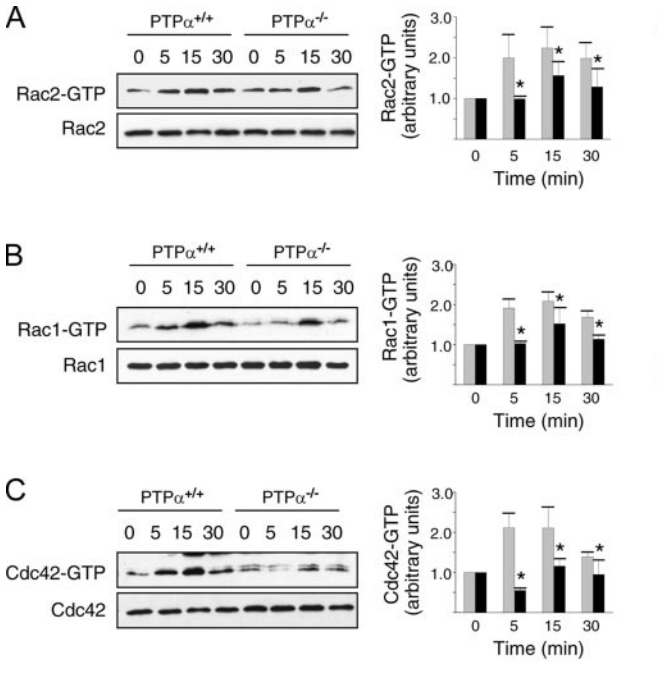

FIGURE 7. **Reduced Rac and Cdc42 activation by SCF in PTPα$^{-/-}$ BMMCs.** Wild-type (PTPα$^{+/+}$) and PTPα$^{-/-}$ BMMCs were left untreated (0) or stimulated with SCF for 5, 15, and 30 min. Lysates were used for GST-PBD binding assays, and the GST-PBD complexes (*upper panels*) and cell lysates (*lower panels*) were analyzed by immunoblotting for Rac2 (*A*), Rac1 (*B*), and Cdc42 (*C*). Independent pulldown assays were used to detect activated Rac2, Rac1, and Cdc42. *D*, cell lysates were probed for phospho-PAK and PAK. *E*, Vav1 immunoprecipitates were probed for phosphotyrosine (*P-Tyr*) and Vav1. The results of several experiments (Rac2, Rac1, Cdc42, and PAK, $n = 3$; Vav1, $n = 4$) were quantified by densitometry, and are shown as mean ± S.D. in the *bar graphs*. *Asterisks* indicate a significant difference ($p < 0.05$) between wild-type (*gray bars*) and PTPα$^{-/-}$ (*black bars*) cells.

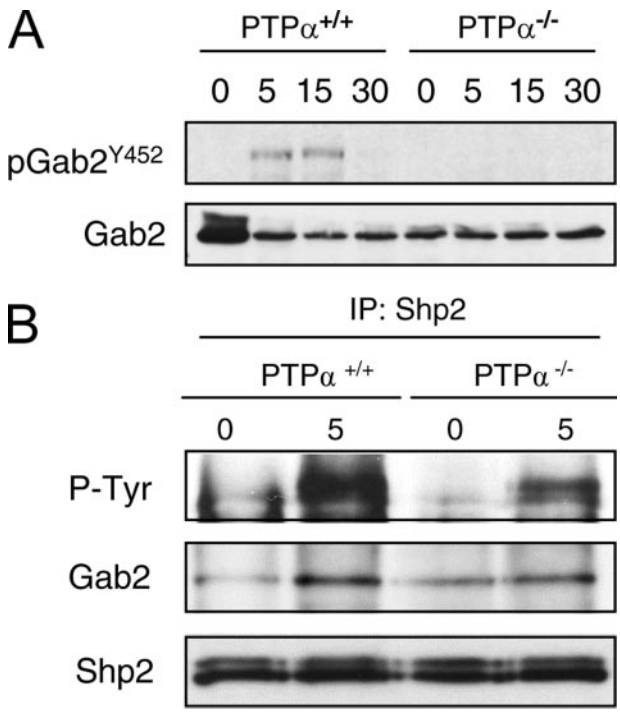

FIGURE 8. **Aberrant SCF-induced Gab2 phosphorylation in PTPα$^{-/-}$ BMMCs.** Wild-type (PTPα$^{+/+}$) and PTPα$^{-/-}$ BMMCs were untreated (0) or stimulated with SCF for 5, 15, and 30 min. *A*, cell lysates were probed with antibodies to phospho-Tyr^{452}-Gab2 and Gab2. The results shown are representative of those obtained in two other independent experiments. *B*, Shp2 immunoprecipitates (*IP*) were probed with antibodies to phosphotyrosine (*P-Tyr*), Gab2, and Shp2. The phosphotyrosyl proteins detected in the *top panel* co-migrate with Shp2. Similar results were obtained in another independent experiment.

Cdc42 effector PAK was impaired. We detected no increase in PAK phosphorylation at 5 min and reduced PAK phosphorylation at 15 and 30 min of SCF treatment of PTPα$^{-/-}$ cells (Fig. 7*D*). The SCF-induced activation of Vav (47), an upstream activator of Rac, was also significantly reduced at 15 and 30 min in PTPα$^{-/-}$ cells (Fig. 7*E*).

Gab2 and Shp2 Phosphorylation Is Impaired in SCF-stimulated PTPα$^{-/-}$ BMMCs—Shc binds to phospho-Tyr^{567} of activated c-Kit and is tyrosine phosphorylated by a non-SFK-type kinase (33, 46). This promotes the association of Shc with Grb2, and via Grb2, with Gab2. The c-Kit-associated Gab2 is tyrosine phosphorylated by SFKs, allowing the recruitment and phosphorylation of Shp2 that is necessary for downstream activation of Rac/JNK (46). We therefore examined whether SCF-stimulated Gab2 phosphorylation is affected in the absence of PTPα. In wild-type BMMCs, SCF-induced phosphorylation of Gab2 at Tyr^{452} was detectable at 5 and 15 min and disappeared by 30 min. However, in PTPα-null BMMCs, no phosphorylation of Gab2 at this site was observed at any time up to 30 min of SCF treatment (Fig. 8*A*). Shp2 is activated by tyrosine phosphorylation, although the mechanism by which Gab2-associated Shp2 signals to Rac/JNK is unknown. SCF-stimulated Shp2 phosphorylation was also reduced in PTPα-null BMMCs, as was its association with Gab2 (Fig. 8*B*). The above results indicate that SCF-stimulated Gab2 phosphorylation is mediated by PTPα, and that defective Gab2/Shp2 phosphorylation and signaling in SCF-stimulated PTPα$^{-/-}$ BMMCs could result in the impaired Rac and JNK activation observed in these cells.

Re-expression of PTPα Rescues c-Kit Signaling Defects—PTPα$^{-/-}$ BMMCs were infected with retrovirus expressing PTPα or a control "empty" vector (Fig. 9*A*). The re-expression of PTPα (to 147% of the level in wild-type BMMCs) restored SCF-induced c-Kit phosphorylation at Tyr$^{567/569}$ and Tyr^{719} to levels observed in wild-type BMMCs, whereas PTPα$^{-/-}$ BMMCs infected with virus containing the empty vector still exhibited reduced c-Kit phosphorylation at these sites (Fig. 9*B*). The SCF-stimulated phosphorylation and activation of the downstream signaling molecules ERK1/2 and p38 (Fig. 9*C*) were also restored to normal levels in PTPα$^{-/-}$ BMMCs upon PTPα re-expression, confirming that the c-Kit signaling defects observed in the PTPα-null cells were indeed entirely due to the lack of this receptor phosphatase.

Altered Tissue Distribution of Mast Cells in PTPα$^{-/-}$ Mice—We investigated whether the absence of PTPα affected mast cell populations in specific tissues. No difference in mast cell

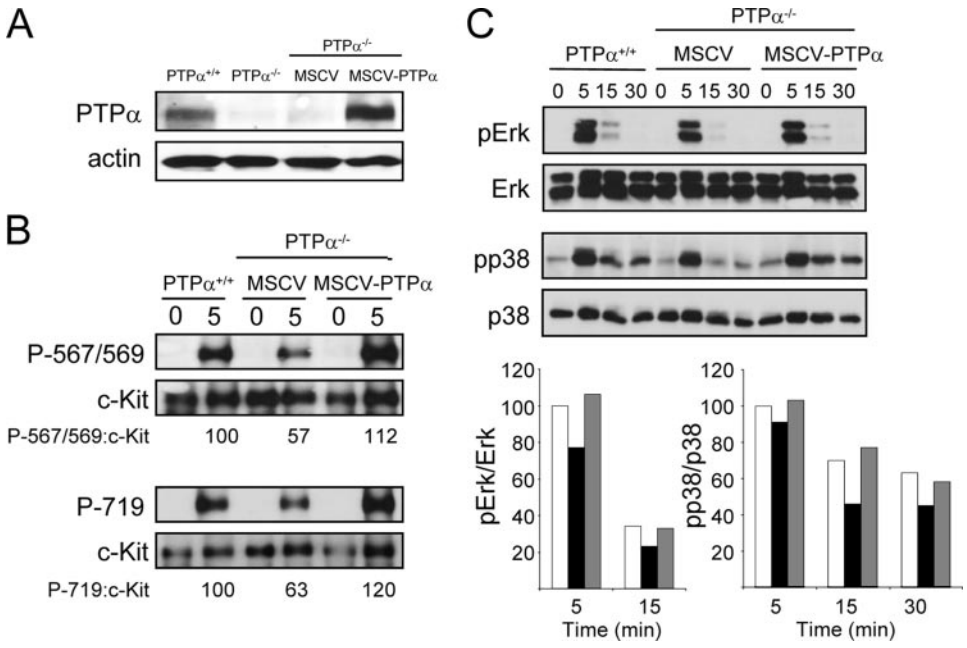

FIGURE 9. **Restoring PTPα expression in PTPα$^{-/-}$ BMMCs rescues c-Kit phosphorylation and MAPK activation defects.** PTPα$^{+/+}$ and PTPα$^{-/-}$ BMMCs, and PTPα$^{-/-}$ BMMCs that had been infected with MSCV bearing empty vector (*MSCV*) or a PTPα expression vector (*MSCV-PTPα*) were left unstimulated or treated with SCF for the indicated times (min) and lysed. *A*, unstimulated lysates were probed for PTPα and actin. *B*, lysates were probed for phospho-Tyr$^{567/569}$ and phospho-Tyr^{719} of c-Kit, and for c-Kit. The signals were quantified from this and another independent experiment and averaged, and are shown under the autoradiographs as % phosphorylation for the sites (with wild-type cells taken as 100%). *C*, lysates were probed for phospho-ERK and ERK, and phospho-p38 and p38. Quantified signals from this and another independent experiment were averaged and are depicted in the graphs as % phosphorylation relative to that in wild-type cells (taken as 100% at 5 min). *White bars*, wild-type BMMCs; *black bars*, PTPα-null BMMCs with MSCV empty vector; *gray bars*, PTPα-null BMMCs with MSCV expressing PTPα. Due to the high signals detected at 5 min *versus* the much lower signals at later time points, quantification of the 5-min signals was made at a non-linear exposure and underrepresents differences between the cell types.

number was found in the dermis of back skin, but mast cell numbers were significantly reduced in the hypodermis of the back skin and in the ears of PTPα-deficient mice compared with wild-type mice (Fig. 10, *A–C*). Peritoneal cells were collected by lavage, and FACS analyzed for c-Kit- and FcεR1-positive mast cells. Although total peritoneal cell numbers did not differ between genotypes, a striking 2-fold increase in the absolute number of mast cells was found in the PTPα$^{-/-}$ mice (Fig. 10*D*). Similar results were obtained by counting toluidine blue-positive mast cells and total cells collected from peritoneal lavages (data not shown). The same alterations were found in these tissues and for peritoneal mast cell percentages of wild-type and PTPα-null C57Bl6 mice (recently obtained after 10 generations of backcrossing the 129*SvEv* PTPα$^{-/-}$ animals) (data not shown), indicating that differences in tissue mast cells numbers are due to the ablation of PTPα and not to the mixed genetic background of the 129EvSv x Black Swiss mice. As the above represent connective tissue-type mast cells, we also examined mast cell numbers in the stomach mucosa but detected no difference in mucosal mast cell numbers between genotype (Fig. 10*E*). However, submucosal mast cells (usually considered as connective tissue mast cells) were significantly reduced in the PTPα$^{-/-}$ mice (Fig. 10*F*).

DISCUSSION

This study has identified PTPα as a critical determinant of the ability of mast cells to migrate and polarize in response to the c-Kit ligand SCF. PTPα regulates integrin signaling and migration in fibroblasts, however, the minimal migration of BMMCs that is observed upon integrin stimulation alone coupled with the strong dependence of mast cell migration on SCF prompted us to investigate the mechanisms of PTPα regulation of SCF/c-Kit signaling in BMMCs.

We demonstrate that PTPα plays an important role in immediate events triggered upon binding of SCF to c-Kit, as two key early changes, c-Kit phosphorylation and SFK activation, are impaired in the absence of PTPα. In PTPα$^{-/-}$ BMMCs there is reduced phosphorylation of c-Kit at Tyr$^{567/569}$ and Tyr^{719}, and defective activation of Fyn. Although Fyn-dependent phosphorylation of c-Kit at specific sites has not been examined, the overall tyrosine phosphorylation of c-Kit is unaffected in Fyn-deficient BMMCs (39), and this is similar to our observations in PTPα$^{-/-}$ BMMCs. Total and site-specific SCF-stimulated c-Kit tyrosine phosphorylation is reduced in Lyn-deficient BMMCs (41). SCF-stimulated Lyn phosphorylation/activation was not detectably altered in the absence of PTPα. However, neither did we observe altered Lyn phosphorylation/activation in SCF-treated wild-type BMMCs, and thus we are unable to draw any conclusions about the PTPα-mediated regulation of Lyn in c-Kit signaling. We found that phosphorylation of c-Kit at Tyr$^{567/569}$ and Tyr^{719} is also reduced in BMMCs treated with the SFK inhibitor SU6656, indicating that the loss of PTPα-mediated Fyn activation, and perhaps that of other SFKs, is likely the critical defect underlying the reduced site-specific phosphorylation of c-Kit in PTPα-null BMMCs.

Despite reduced phosphorylation of c-Kit at its PI3K binding site, Tyr^{719}, PI3K/Akt signaling was not affected in PTPα$^{-/-}$ BMMCs. In other studies, SCF-treated Fyn-null or Lyn-null BMMCs likewise did not exhibit altered binding of the p85 subunit of PI3K to c-Kit nor reduced Akt activation, although reduced phosphorylation of c-Kit at both Tyr$^{567/569}$ and Tyr^{719} was observed in the latter cell type (39, 41). Because either of these important c-Kit phosphorylation sites can mediate PI3K and Akt activation in the absence of the other site (32), it appears that the partial phosphorylation of both sites in PTPα-null BMMCs (as in the Lyn-null cells) is sufficient for SCF-stimulated PI3K/Akt signaling.

However, in contrast to PI3K/Akt signaling, the SCF-induced activation of several other signaling molecules was defective in the absence of PTPα, including the scaffolding molecule Gab2. Gab2 functions downstream of SFK-mediated c-Kit sig-

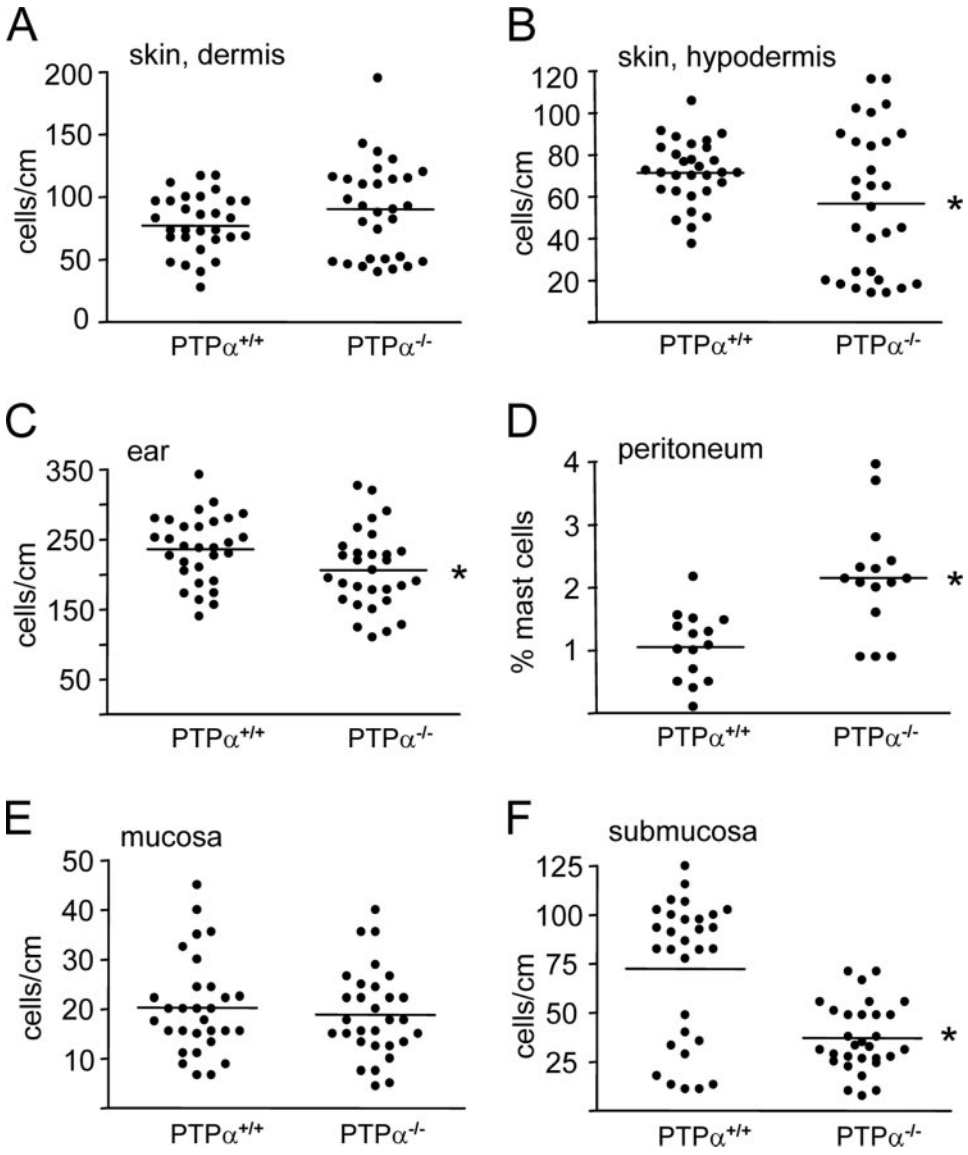

FIGURE 10. **Distribution of mast cells in wild-type and PTPα-null mouse tissues.** Toluidine blue-stained mast cells were counted in the dermis (*A*) and hypodermis of back skin sections (*B*), in ear sections (*C*), and in sections of stomach mucosa (*E*) and submucosa (*F*) of tissues from wild-type ($PTP\alpha^{+/+}$) and PTPα-null ($PTP\alpha^{-/-}$) mice. Mast cell numbers were counted in 10 sections of each tissue sample from each of three mice of each genotype, and are represented as cells/cm of tissue. *D*, cells obtained by peritoneal lavage from mice of each genotype ($n = 15$) were FACS analyzed for c-Kit- and FcεR1-positive mast cells, and for total cell number. The mast cell percentage of the total cell number is shown. All data were analyzed using analysis of variance. *Horizontal lines* represent the means, and significant differences between genotypes in the hypodermis and ear ($p < 0.05$) and in the peritoneum and sub-mucosa ($p < 0.01$) are indicated by the *asterisks*.

naling, as the mutation of Tyr^{567} inhibits Gab2 tyrosine phosphorylation and association with c-Kit, and inhibition of SFKs strongly reduces SCF-induced Gab2 tyrosine phosphorylation (46). It has been proposed that, upon recruitment to c-Kit via Shc/Grb2 binding, Gab2 is phosphorylated by c-Kit-associated SFKs (46). Our finding that SCF-stimulated Gab2 tyrosine phosphorylation is abrogated in $PTP\alpha^{-/-}$ BMMCs that have impaired Fyn activity is consistent with this, and place PTPα as an upstream player in signaling from c-Kit to Fyn to Gab2, with PTPα functioning in conjunction with c-Kit to stimulate Fyn activity.

Previous studies have found that c-Kit $Tyr^{567/569}$, Fyn, and Gab2 are involved in the SCF-dependent activation of Rac/JNK signaling, and of ERK1/2 and p38. Mutation of the c-Kit $Tyr^{567/569}$ SFK binding site reduces Rac and JNK activation, and mutation of Tyr^{567} reduces activation of p38 and the ERK1/2 activating kinase mitogen-activated protein kinase/extracellular signal-regulated kinase kinase (MEK) 1/2 (31, 34). Restoration of $Tyr^{567/569}$ to c-Kit devoid of other major sites of tyrosine phosphorylation rescues ligand-stimulated Fyn, Rac, JNK, and ERK1/2 activation (32). In addition, mast cells lacking Fyn show defective activation of Rac1, Rac2, JNK, and p38 (39, 40), and those lacking Gab2 show defective activation of Rac1, Rac2, JNK, and ERK (46, 48). Overall, there is strong evidence for SFK signaling from c-Kit to Gab2, resulting in the downstream activation of Rac/JNK, p38, and ERK1/2. Our studies with $PTP\alpha^{-/-}$ BMMCs indicate that PTPα is required for effective SCF-induced activation of Rac1 and -2, and of the MAPKs JNK, p38, and ERK1/2, likely as a consequence of the action of PTPα as an activator of Fyn, and at least for some of these events, of Fyn-Gab2 signaling. We have also demonstrated that PTPα plays a role in SCF-induced activation of Vav, PAK, and Cdc42, proteins that can function as intermediates in these signaling pathways.

SFKs are critical for mast cell migration, as expression of the SFK inhibitory kinase Csk inhibits SCF-induced migration (31). Fyn-null BMMCs exhibit defective SCF-induced spreading and lamellipodia formation that is not observed in Lyn-null BMMCs (47), whereas both Fyn-null and Lyn-null BMMCs have impaired SCF-stimulated migratory ability (39, 40, 42). The impaired SCF-induced spreading, polarization, and migration of $PTP\alpha^{-/-}$ BMMCs are in accord with the defective Fyn activation observed in these cells. Our results indicate that PTPα is specifically required for the activation of a Fyn-based arm (Fyn/Gab2/Shp2/Vav/PAK/Rac/JNK) of c-Kit-mediated signaling that mediates mast cell migration and chemotaxis.

The impaired c-Kit-dependent motility of $PTP\alpha^{-/-}$ BMMCs may be manifested in the altered tissue resident mast cell numbers that we observe in PTPα-null mice. Indeed, c-Kit phosphorylation and c-Kit-linked signaling molecules that are functionally impaired in $PTP\alpha^{-/-}$ BMMCs have effects, some

profound, on mast cell tissue populations. Mice with c-Kit mutations of Tyr^{567}, $Tyr^{567/569}$, or Tyr^{719}, or deficient in Gab2 or p85α of class I_A PI3K, exhibit reduced or absent mast cells in skin, peritoneum, and/or stomach mucosa and other gastrointestinal regions (43, 46, 48–50). Fyn-null mice have unaltered numbers of skin mast cells (51), whereas Lyn-null mice are unique in having 2–3-fold more skin and peritoneal mast cells (51, 52). However, none of these mutant mice share the phenotype of PTPα-null mice where some tissues exhibit reduced mast cell populations (hypodermis, ear, and stomach submucosa) but elevated mast cell numbers are present at another site, the peritoneum. Although the basis of this differential effect of ablating PTPα is unknown, we speculate that besides migration, other PTPα-dependent events in mast cell proliferation, survival, development, and/or maturation could affect mast cell populations in tissue-specific manners. Furthermore, additional or alternative actions of PTPα, as a plasma membrane mast cell receptor, might regulate other (non-c-Kit) signaling pathways in tissue- or developmentally specific manners that differentially combine with its actions on c-Kit signaling to determine mast cell populations.

Collectively, our findings establish that PTPα plays an upstream positive regulatory role in c-Kit signaling and BMMC migration, and regulates tissue mast cell populations *in vivo*, highlighting the importance of PTPα in the function of these immune cells. Specifically, PTPα mediates activation of the SFK Fyn in response to the c-Kit ligand SCF. As c-Kit and SFK inhibitors have shown therapeutic utility in the treatment of some forms of cancer (29, 53), our findings have implications for targeting PTPα as an additional or alternate strategy in the treatment of diseases that are associated with up-regulated SFK-dependent c-Kit signaling.

Acknowledgments—We are grateful to Dr. Andrew Craig of Queen's University for the gift of X63-IL-3 cells and for helpful advice and critical reading of the manuscript. We also thank Darrell Bessette for comments on the manuscript, Dr. Kelly McNagy of the University of British Columbia for providing WEHI-3 cells, and Dr. Ed Manser of the Institute of Molecular and Cell Biology, Singapore, for pGEX-PBD. Maintenance of the PTPα$^{-/-}$ mouse colony by Dr. Jing Wang is gratefully acknowledged.

REFERENCES

1. Pallen, C. J. (2003) *Curr. Top. Med. Chem.* **3,** 821–835
2. Zheng, X. M., Wang, Y., and Pallen, C. J. (1992) *Nature* **359,** 336–339
3. den Hertog, J., Pals, C. E., Peppelenbosch, M. P., Tertoolen, L. G., de Laat, S. W., and Kruijer, W. (1993) *EMBO J.* **12,** 3789–3798
4. Su, J., Muranjan, M., and Sap, J. (1999) *Curr. Biol.* **9,** 505–511
5. Ponniah, S., Wang, D. Z., Lim, K. L., and Pallen, C. J. (1999) *Curr. Biol.* **9,** 535–538
6. Petrone, A., Battaglia, F., Wang, C., Dusa, A., Su, J., Zagzag, D., Bianchi, R., Casaccia-Bonnefil, P., Arancio, O., and Sap, J. (2003) *EMBO J.* **22,** 4121–4131
7. Skelton, M. R., Ponniah, S., Wang, D. Z., Doetschman, T., Vorhees, C. V., and Pallen, C. J. (2003) *Brain Res.* **984,** 1–10
8. Lei, G., Xue, S., Chery, N., Liu, Q., Xu, J., Kwan, C. L., Fu, Y. P., Lu, Y. M., Liu, M., Harder, K. W., and Yu, X. M. (2002) *EMBO J.* **21,** 2977–2989
9. Le, H. T., Maksumova, L., Wang, J., and Pallen, C. J. (2006) *J. Neurochem.* **98,** 1798–1809
10. Tsai, W., Morielli, A. D., Cachero, T. G., and Peralta, E. G. (1999) *EMBO J.* **18,** 109–118
11. Tiran, Z., Peretz, A., Sines, T., Shinder, V., Sap, J., Attali, B., and Elson, A. (2006) *Mol. Biol. Cell* **17,** 4330–4342
12. Bodrikov, V., Leshchyns'ka, I., Sytnyk, V., Overvoorde, J., den Hertog, J., and Schachner, M. (2005) *J. Cell Biol.* **168,** 127–139
13. Kostic, A., Sap, J., and Sheetz, M. P. (2007) *J. Cell Sci.* **120,** 3895–3904
14. Yang, L. T., Alexandropoulos, K., and Sap, J. (2002) *J. Biol. Chem.* **277,** 17406–17414
15. Ye, H., Tan, Y. L., Ponniah, S., Takeda, Y., Wang, S. Q., Schachner, M., Watanabe, K., Pallen, C. J., and Xiao, Z. C. (2008) *EMBO J.* **27,** 188–200
16. Zeng, L., Si, X., Yu, W. P., Le, H. T., Ng, K. P., Teng, R. M., Ryan, K., Wang, D. Z., Ponniah, S., and Pallen, C. J. (2003) *J. Cell Biol.* **160,** 137–146
17. Maksumova, L., Le, H. T., Muratkhodjaev, F., Davidson, D., Veillette, A., and Pallen, C. J. (2005) *J. Immunol.* **175,** 7947–7956
18. Zheng, X. M., and Shalloway, D. (2001) *EMBO J.* **20,** 6037–6049
19. Zeng, L., D'Alessandri, L., Kalousek, M. B., Vaughan, L., and Pallen, C. J. (1999) *J. Cell Biol.* **147,** 707–714
20. von Wichert, G., Jiang, G., Kostic, A., De Vos, K., Sap, J., and Sheetz, M. P. (2003) *J. Cell Biol.* **161,** 143–153
21. Maksumova, L., Wang, Y., Wong, N. K., Le, H. T., Pallen, C. J., and Johnson, P. (2007) *J. Biol. Chem.* **282,** 20925–20932
22. Brown, J. M., Wilson, T. M., and Metcalfe, D. D. (2008) *Clin. Exp. Allergy* **38,** 4–18
23. Kovanen, P. T. (2007) *Immunol. Rev.* **217,** 105–122
24. Sayed, B. A., Christy, A., Quirion, M. R., and Brown, M. A. (2008) *Annu. Rev. Immunol.* **26,** 705–739
25. Kitamura, Y. (1989) *Annu. Rev. Immunol.* **7,** 59–76
26. Galli, S. J., Kalesnikoff, J., Grimbaldeston, M. A., Piliponsky, A. M., Williams, C. M., and Tsai, M. (2005) *Annu. Rev. Immunol.* **23,** 749–786
27. Okayama, Y., and Kawakami, T. (2006) *Immunol. Res.* **34,** 97–115
28. Lennartsson, J., Jelacic, T., Linnekin, D., and Shivakrupa, R. (2005) *Stem Cells* **23,** 16–43
29. Orfao, A., Garcia-Montero, A. C., Sanchez, L., and Escribano, L. (2007) *Br. J. Haematol.* **138,** 12–30
30. Renneville, A., Roumier, C., Biggio, V., Nibourel, O., Boissel, N., Fenaux, P., and Preudhomme, C. (2008) *Leukemia* **22,** 915–931
31. Ueda, S., Mizuki, M., Ikeda, H., Tsujimura, T., Matsumura, I., Nakano, K., Daino, H., Honda Zi, Z., Sonoyama, J., Shibayama, H., Sugahara, H., Machii, T., and Kanakura, Y. (2002) *Blood* **99,** 3342–3349
32. Hong, L., Munugalavadla, V., and Kapur, R. (2004) *Mol. Cell. Biol.* **24,** 1401–1410
33. Price, D. J., Rivnay, B., Fu, Y., Jiang, S., Avraham, S., and Avraham, H. (1997) *J. Biol. Chem.* **272,** 5915–5920
34. Timokhina, I., Kissel, H., Stella, G., and Besmer, P. (1998) *EMBO J.* **17,** 6250–6262
35. Linnekin, D., DeBerry, C. S., and Mou, S. (1997) *J. Biol. Chem.* **272,** 27450–27455
36. Price, D. J., Rivnay, B., and Avraham, H. (1999) *Biochem. Biophys. Res. Commun.* **259,** 611–616
37. Ronnstrand, L. (2004) *Cell Mol. Life Sci.* **61,** 2535–2548
38. Roskoski, R., Jr. (2005) *Biochem. Biophys. Res. Commun.* **337,** 1–13
39. Samayawardhena, L. A., Hu, J., Stein, P. L., and Craig, A. W. (2006) *Cell Signal.* **18,** 1447–1454
40. Samayawardhena, L. A., Kapur, R., and Craig, A. W. (2007) *Blood* **109,** 3679–3686
41. Shivakrupa, R., and Linnekin, D. (2005) *Cell Signal.* **17,** 103–109
42. O'Laughlin-Bunner, B., Radosevic, N., Taylor, M. L., Shivakrupa, DeBerry, C., Metcalfe, D. D., Zhou, M., Lowell, C., and Linnekin, D. (2001) *Blood* **98,** 343–350
43. Fukao, T., Yamada, T., Tanabe, M., Terauchi, Y., Ota, T., Takayama, T., Asano, T., Takeuchi, T., Kadowaki, T., Hata Ji, J., and Koyasu, S. (2002) *Nat. Immunol.* **3,** 295–304
44. Tan, B. L., Yazicioglu, M. N., Ingram, D., McCarthy, J., Borneo, J., Williams, D. A., and Kapur, R. (2003) *Blood* **101,** 4725–4732
45. Serve, H., Hsu, Y. C., and Besmer, P. (1994) *J. Biol. Chem.* **269,** 6026–6030
46. Yu, M., Luo, J., Yang, W., Wang, Y., Mizuki, M., Kanakura, Y., Besmer, P., Neel, B. G., and Gu, H. (2006) *J. Biol. Chem.* **281,** 28615–28626

47. Alai, M., Mui, A. L., Cutler, R. L., Bustelo, X. R., Barbacid, M., and Krystal, G. (1992) *J. Biol. Chem.* **267,** 18021–18025
48. Nishida, K., Wang, L., Morii, E., Park, S. J., Narimatsu, M., Itoh, S., Yamasaki, S., Fujishima, M., Ishihara, K., Hibi, M., Kitamura, Y., and Hirano, T. (2002) *Blood* **99,** 1866–1869
49. Agosti, V., Corbacioglu, S., Ehlers, I., Waskow, C., Sommer, G., Berrozpe, G., Kissel, H., Tucker, C. M., Manova, K., Moore, M. A., Rodewald, H. R., and Besmer, P. (2004) *J. Exp. Med.* **199,** 867–878
50. Kimura, Y., Jones, N., Kluppel, M., Hirashima, M., Tachibana, K., Cohn, J. B., Wrana, J. L., Pawson, T., and Bernstein, A. (2004) *Proc. Natl. Acad. Sci. U. S. A.* **101,** 6015–6020
51. Odom, S., Gomez, G., Kovarova, M., Furumoto, Y., Ryan, J. J., Wright, H. V., Gonzalez-Espinosa, C., Hibbs, M. L., Harder, K. W., and Rivera, J. (2004) *J. Exp. Med.* **199,** 1491–1502
52. Hernandez-Hansen, V., Mackay, G. A., Lowell, C. A., Wilson, B. S., and Oliver, J. M. (2004) *J. Leukocyte Biol.* **75,** 143–151
53. Apice, G., Milano, A., Bruni, G. S., Iaffaioli, R. V., and Caponigro, F. (2006) *Rev. Recent Clin. Trials* **1,** 35–42